Optical response of a nematic liquid crystal cell at the splay - bend transition: a model and dynamic simulation

Peizhi Xu[a]; Vladimir Chigrinov[a]; Alexei D. Kiselev[a]

[a] Hong Kong University of Science and Technology, Clear Water Bay, Hong Kong

PLEASE SCROLL DOWN FOR ARTICLE

Optical response of a nematic liquid crystal cell at the splay – bend transition: a model and dynamic simulation

PEIZHI XU*, VLADIMIR CHIGRINOV and ALEXEI D. KISELEV

Hong Kong University of Science and Technology, Clear Water Bay, Kowloon, Hong Kong

We study the dynamical optical response of a nematic liquid crystal cell that undergoes the splay–bend transition after applying a voltage across the cell. We formulate a simplified model that takes into account both the flexoelectric coupling and the surface rotational viscosity. The dynamic equations of the model are solved numerically to calculate the temporal evolution of the director profile and of the transmittance. We evaluate the response time as a function of a number of parameters, such as dielectric and elastic anisotropies, asymmetry of the surface pretilt angles, anchoring energy, surface rotational viscosity and flexoelectricity.

1. Introduction

As originally shown by Berreman and Heffner [1], a nematic liquid crystal (NLC) cell can be prepared in two metastable states that can be switched either way by applying an electric field. This general idea underlies the mode of operation of bistable liquid crystal devices that have attracted considerable attention in recent decades.

The approach pioneered in [1] is based on using bistable twisted NLC cells that have two metastable twist states produced as a result of a mismatch between the NLC pitch and the twist imposed by the boundary conditions at the substrates. This approach has been extensively studied and found to have difficulties arising from the fast relaxation of the metastable states to the intermediate stable configuration [2–6].

An alternative approach is to use the so-called optically compensated bend NLC cells also known as π cells [7–11]. The boundary surfaces of such cells favour a uniformly tilted alignment and the pretilt angles at the substrates are equal in magnitude but opposite in sign. For sufficiently large surface pretilt angles, the equilibrium orientational structures are non-twisted [7, 8, 12, 13] and there are two director configurations that under certain conditions are degenerate in energy: the splay (horizontal) state and the bend (vertical) state.

In contrast to the bistable twisted cells, these bistable states are topologically distinct and separated by an energy barrier. Thus, the splay and bend states are both stable in the long term. Applying a voltage across the cell can switch the splay state to the bend state. This splay–bend transition will be our primary concern, and here we report a study of the dynamics of a NLC cell that undergoes the splay–bend transition induced by an external electric field.

The dynamical theory of NLC systems, so-called nematohydrodymanics, is very complicated and the dynamical properties of bistable liquid crystal cells have yet to receive much attention. In recent theoretical studies of the dynamics of π cells [14], zenithally bistable [15] and super-twisted [16] NLC devices were investigated using different simplified models.

In this paper we focus on the optical response of a NLC cell after switching-on the voltage. The corresponding response time will be studied as a function of a number of factors such as dielectric and elastic anisotropies, asymmetry of the surface pretilt angles, anchoring strengths, surface rotational viscosity and flexoelectricity. In §2 we formulate our model and derive a set of dynamic equations. The numerical results are presented in §3. Concluding remarks are given in §4.

2. The model

In this section we describe our model and derive a set of dynamic equations. These equations will then be used to simulate the orientational dynamics of a NLC layer of thickness d that undergoes the splay–bend transition under the action of an electric field.

*Corresponding author. Email: pazixu@ust.hk

2.1. *Free energy*

The layer is sandwiched between two parallel plates, $z=0$ (lower substrate) and $z=d$ (upper substrate), and we assume that both the electric field, $\mathbf{E}$, and the z-axis are normal to the plane of the substrates. In addition, and similar to [14, 15, 17, 18], we shall restrict our consideration to the case in which the splay–bend transition does not involve twisted states. In this case, the NLC director field, $\mathbf{n}$, is constrained to lie in the xz-plane:

$$\mathbf{n} = \cos \theta(z)\mathbf{e}_x + \sin \theta(z)\mathbf{e}_z \qquad (1)$$

where θ is the tilt angle defined as the angle between the plane of the boundary surfaces and the director; $\mathbf{e}_x$ and $\mathbf{e}_z$ are the unit vectors parallel to the x-axis and the z-axis, respectively.

The vectors of easy orientation at the lower and the upper substrates are similarly characterised by the tilt angles θ_L and $-\theta_U$, respectively. Thus, the anchoring energy per unit area taken in the Rapini–Papoular form [19] is

$$f_{\text{anch}} = \frac{W_L}{2}\sin^2(\theta_0 - \theta_L) + \frac{W_U}{2}\sin^2(\theta_1 + \theta_U) \qquad (2)$$

where $\theta_{0,1} = \theta|_{z=0,d}$ and W_L (W_U) is the strength of anchoring at the lower (upper) substrate. We shall also need to write the bulk part of the free energy per unit area as,

$$F_b[\mathbf{n}, \mathbf{E}] = F_{\text{el}}[\mathbf{n}] + F_E[\mathbf{n}, \mathbf{E}] \qquad (3)$$

which is a sum of the Frank elastic energy, $F_{\text{el}}[\mathbf{n}]$, and the energy of interaction between NLC molecules and the electric field, $F_E[\mathbf{n}, \mathbf{E}]$.

For the director distribution (1), using the standard expression for the Frank elastic energy [20] gives:

$$F_{\text{el}}[\theta] = \frac{1}{2}\int_0^d K_{\text{el}}(\theta)\dot{\theta}^2\,\mathrm{d}z,$$

where the $\cdot$ indicates the derivative with respect to z and $K_{\text{el}}(\theta) = K_{11}\cos^2\theta + K_{33}\sin^2\theta$ is the effective angle-dependent elastic coefficient; K_{11} and K_{33} are the splay and bend elastic constants, respectively. Similarly, the director field (1) can be used to derive the expression for the electrostatic energy $F_E[\mathbf{n}, \mathbf{E}]$ that depends on the electric field: $\mathbf{E} = E_z\mathbf{e}_z$.

Assuming that the NLC Debye screening length is larger than the layer thickness, the NLC material can be regarded as an insulator. Thus, we can neglect the effects caused by the presence of ionic charges. However, the flexoelectric coupling between the NLC and the applied field cannot be generally disregarded. This coupling is known to be caused by splay and bend

director distortions that give rise to an average flexoelectric polarization,

$$\mathbf{P}_f = e_{11}\mathbf{n}(\nabla\cdot\mathbf{n}) + e_{33}(\mathbf{n}\cdot\nabla)\mathbf{n} \qquad (5)$$

characterized by the splay and bend flexoelectric coefficients, e_{11} and e_{33}. This is the well known flexoelectric effect, first described by Meyer [21], which has been extensively studied in recent years. Flexoelectricity appears to be a very important property of NLCs which must be taken into account in all experiments that deal with inhomogeneous director orientations.

In our case, it is not difficult, from equation (4), to obtain the z-component of the flexoelectric polarization (5) in the following form:

$$P_z = g(\theta)\dot{\theta}, \quad g(\theta) = e_f\sin\theta\cos\theta \qquad (6)$$

where $e_f = e_{11} + e_{33}$ is the flexoelectric coefficient. Thus, the final result for the electrostatic energy is

$$F_E[\theta, E_z] = -\int_0^d \left[\varepsilon_{zz}E_z^2/2 + P_zE_z\right]\mathrm{d}z \qquad (7)$$

$$\varepsilon_{zz}(\theta) = \varepsilon_\perp\left(1 + u\sin^2\theta\right) \qquad (8)$$

where $\varepsilon_{ij} = \varepsilon_\perp\delta_{ij} + (\varepsilon_\parallel - \varepsilon_\perp)n_in_j$ is the dielectric tensor and $u = (\varepsilon_\parallel - \varepsilon_\perp)/\varepsilon_\perp$ is the dielectric anisotropy parameter.

The Maxwell equation $\nabla\times\mathbf{E} = 0$ implies that the electric field $\mathbf{E} = E_z(z)\mathbf{e}_z$ can be expressed in terms of the scalar potential, $V : E_z = -\dot{V}$. Variation of the electrostatic energy functional (7) with respect to V gives the well known electrostatic constitutive relation

$$-\frac{\delta F_E}{\delta E_z} = \varepsilon_{zz}E_z + P_z = D_z \qquad (9)$$

where D_z is the z-component of the electric displacement field that, in contrast to E_z, does not depend on z.

From equation (9) the displacement D_z can be expressed in terms of the voltage $U = \int_0^d E_z\,\mathrm{d}z = V(0) - V(d)$ as

$$D_z = \frac{U + \psi(\theta_1) - \psi(\theta_0)}{\int_0^d \varepsilon_{zz}^{-1}(\theta)\mathrm{d}z} \qquad (10)$$

where

$$\psi(\theta) = \int g(\theta)\varepsilon_{zz}^{-1}(\theta)\mathrm{d}\theta = \frac{e_f\ln(1 + u\sin^2\theta)}{2u\varepsilon_\perp}.$$

The expression on the right hand side of equation (10) clearly indicates the flexoelectricity-induced voltage shift. The effects of this shift in optical response of hybrid aligned liquid crystal cells have been studied recently [22].

Since the displacement D_z does not vary across the layer, it is convenient to have the displacement D_z as an independent field and use the free energy $G[\theta, D_z]$ which is related to the energy $F[\theta, E_z]$ via the Legendre transformation [23, 24],

$$G[\theta, D_z] = F[\theta, E_z] + E_z D_z \quad (11)$$

where $E_z = (D_z - P_z)/\varepsilon_{zz}$.

We can now combine equations (2)–(4) and (7) to derive the free energy $G[\theta, D_z]$ in the form:

$$G[\theta, D_z] = \int_0^d f_b \, dz + f_s \quad (12)$$

$$f_b = K(\theta) \dot{\theta}^2 + \frac{D_z^2}{\varepsilon_{zz}(\theta)} \quad (13)$$

$$f_s = f_{anch} + D_z[\psi(\theta_0) - \psi(\theta_1)] \quad (14)$$

where $K(\theta) = K_{el}(\theta) + g^2(\theta)/\varepsilon_{zz}(\theta)$ is the effective elastic coefficient renormalized by the flexoelectricity. As can be seen from equations (12)–(14), the bulk elastic coefficient and the anchoring energy are both renormalized by the flexoelectricity: $K_{el} \to K$ and $f_{anch} \to f_s$. The static properties of NLC layers submitted to an electric field are known to be affected by this renormalization [25–29].

2.2. Dynamic equations

Low frequency dynamical properties of NLCs are generally characterized by orientational relaxation as well as by shear and compressional flow. A full set of dynamic equations governing nematohydrodynamics is known as the Ericksen–Leslie equations and describes the temporal evolution of the fluid velocity and director field. When the characteristic time scale of the velocity field is much shorter than the typical time of director reorientation, the flow velocity can be adiabatically eliminated from the dynamics of the NLC. In this approximation, the orientational dynamics is purely relaxational and can be formulated as a time-dependent Ginzburg–Landau model [30, 31]. We shall apply this model to obtain the dynamic equation governing the orientational relaxation of the tilt angle in the bulk. Using the free energy (12) gives,

$$\gamma_b \frac{\partial \theta}{\partial t} = -\frac{\delta G}{\delta \theta}$$
$$= K(\theta)\ddot{\theta} + \frac{1}{2}\left\{ K'(\theta)\dot{\theta}^2 + [D_z/\varepsilon_{zz}(\theta)]^2 \varepsilon'_{zz}(\theta) \right\} \quad (15)$$

where γ_b is the bulk rotational viscosity and prime stands for derivatives with respect to θ.

It should be stressed that under certain circumstances the backflow effect caused by the coupling between the fluid flow and the director may considerably affect the dynamical characteristics of NLC cells. Specifically, the so-called 'optical bounce' in twisted cells manifests itself as a dip in transmission of normally incident light after the electric field is turned off [32–34]. But in cases where the twisted states are of minor importance, backflow is found to induce only quantitative changes in the dynamics [14, 34].

By analogy with equation (15), we can write the dynamic equations for the tilt angles, θ_0 and θ_1, at the lower and upper substrates as [15, 18, 35–37]

$$\gamma_s \frac{\partial \theta_i}{\partial t} = (-1)^i K(\theta_i) \dot{\theta}_i - \frac{\partial f_s}{\partial \theta_i}, \quad i = 0, 1 \quad (16)$$

where γ_s is the surface rotational viscosity, which is defined as the ratio of the torque needed to change the director orientation at the surface for a certain angle and the corresponding relaxation velocity [38, 39].

3. Simulation results

In this section we present our numerical results obtained by solving the dynamic quations (15) and (16) numerically. Dependences of the tilt angle on z at specified points in time were computed using the finite difference time domain method. The parameters used in the calculations are listed in the table [40].

In order to study the dynamics of the optical response of the layer, the data representing the temporal evolution of the director profile, which is the tilt angle as a function of z, $\theta(z, t)$, were used as an input for computing the *transmittance* of light through the layer placed between two crossed polarizers. The expression for the transmittance can be derived by using the Jones matrix method [41]. When the director of the LC cell is at $45°$ to the input polarizer, the transmittance, T, is given by [40]

$$T = \sin^2(\Delta\phi/2) \quad (17)$$

Table. Parameters of the model used in the calculations [40].

Parameter	Value	Parameter	Value
K_{11}/N	6.6×10^{-12}	e_{11}/C m^{-1}	-0.95×10^{-11}
K_{33}/K_{11}	3.0	e_{33}/C m^{-1}	-1.35×10^{-11}
d/μm	2.5	$\varepsilon_\perp$	6.3
W/J m^{-2}	4.0×10^{-4}	ε	12.6
θ_L/°	46.0	U/V	20.0
θ_U/°	44.0	n_o	1.5
γ_b/N s m^{-2}	0.1	n_e	1.6
γ_s/N s m^{-1}	3.0×10^{-6}	λ/μm	0.55

$$\Delta\phi = \frac{2\pi}{\lambda} \int_0^d (n_{\text{eff}} - n_{\text{o}})\,\mathrm{d}z \tag{18}$$

$$\frac{1}{n_{\text{eff}}^2} = \frac{\sin^2\theta}{n_{\text{o}}^2} + \frac{\cos^2\theta}{n_{\text{e}}^2} \tag{19}$$

where $\Delta\phi$ is the phase difference between the ordinary and extraordinary ray; λ is the wavelength of the incident light and n_{o} (n_{e}) is the ordinary (extraordinary) refractive index. Thus, we describe the dynamics of optical response by computing the temporal change in the transmittance (17). An important parameter characterizing the rate of change of the transmittance is the *response time*, which is the time taken for the transmittance to increase from 10% to 90%.

We begin with the case in which the flexoelectric effect is neglected and $e_{\text{f}} = 0$. Figure 1 shows how the director profile evolves in time after applying a voltage across the NLC cell. Asymmetric pretilt angles and symmetric surface anchoring energy are used in this calculation. As seen in figure 1, the initial director configuration corresponds to the splay state which gradually transforms into the bend state under the action of the electric field.

We now consider the effects related to the dielectric and elastic anisotropies. The results for various values of the dielectric anisotropy parameter, $u = (\varepsilon_\parallel - \varepsilon_\perp)/\varepsilon_\perp$, and the elastic ratio, K_{33}/K_{11}, are shown in figures 2 and 3, respectively. Figure 2 (*b*) shows that the response time is a non-monotonic function of the dielectric anisotropy parameter and goes through a minimum in the vicinity of $u = 0.8$. By contrast, as shown in
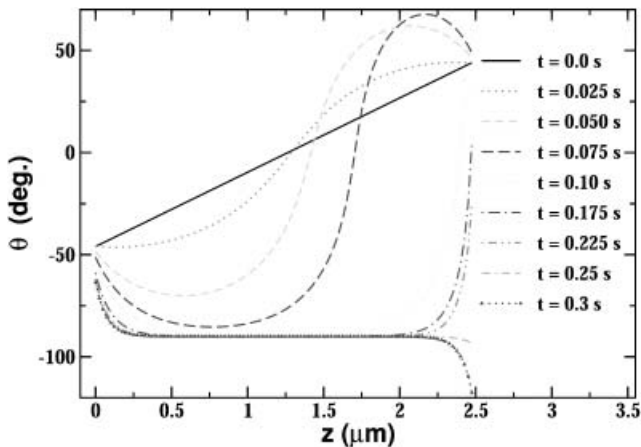
Figure 1. The director configuration through the cell at different points in time after applying the voltage. The anchoring strengths at the substrates are assumed to be equal, $W_{\text{L}} = W_{\text{U}} \equiv W$, and the list of the parameters are given in the table.
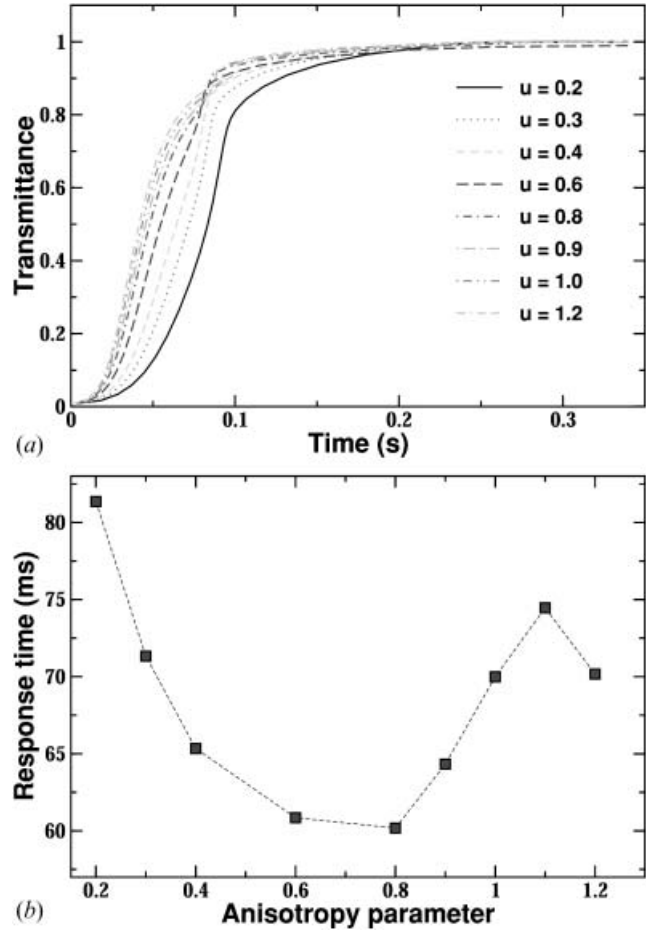
Figure 2. (*a*) Transmittance as a function of time at various values of the dielectric anisotropy parameter, $u = (\varepsilon_\parallel - \varepsilon_\perp)/\varepsilon_\perp$. (*b*) Response time as a function of u.

figure 3 (*b*), the response time monotonically declines as the ratio of K_{33} and K_{11} increases. Thus, large values of the elastic ratio facilitate the splay–bend transition.

The surface pretilt angles, θ_{L} and θ_{U}, are known to play an important part in the splay–bend transition [8]. These are among the parameters that affect the dynamics of the optical response through the boundary conditions at the substrates (16). The first parameter we consider is the difference between the pretilt angles: $\Delta\theta_{\text{s}} = \theta_{\text{L}} - \theta_{\text{U}}$. Figure 4 (*a*) shows the curves for the transmittance varying in time at various values of the pretilt angle difference. As seen in figure 4 (*a*), the curves become steeper as $\Delta\theta_{\text{s}}$ increases and the response time, shown in figure 4 (*b*), is a decreasing function of $\Delta\theta_{\text{s}}$.

The anchoring energy dependence of the response time is plotted in figure 5 for the symmetric case with $W_{\text{L}} = W_{\text{U}} \equiv W$. The curve is shown on a logarithmic scale and clearly indicates the transition between two regimes of anchoring: the weak and the strong anchoring
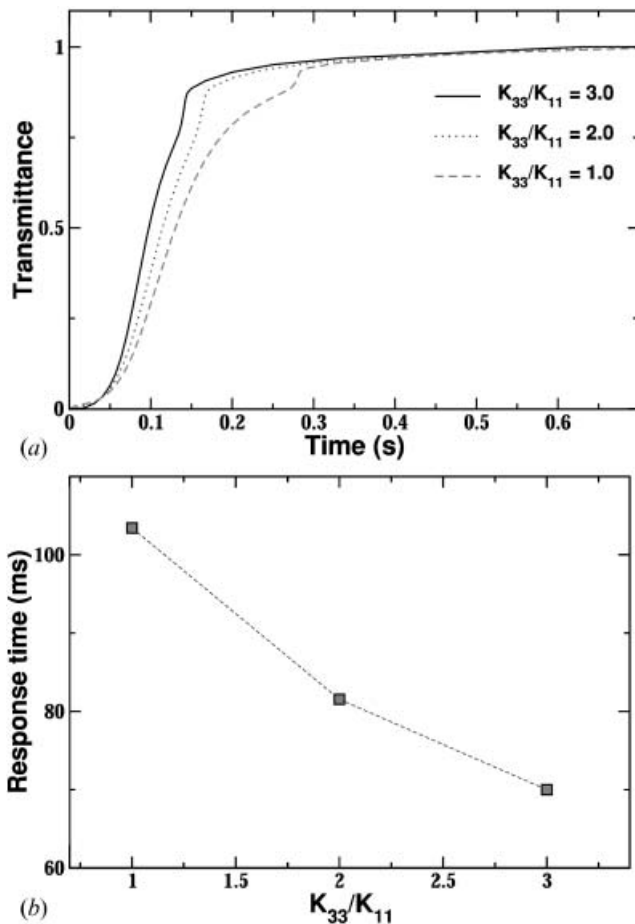
Figure 3. (*a*) Transmittance as a function of time at various values of the elastic ratio K_{33}/K_{11}, $(=\theta_L-\theta_U)$. (*b*) Response time as a function of the elastic ratio K_{33}/K_{11}.

Figure 4. (*a*) Transmittance as a function of time at various values of $\Delta\theta_s$, $(=\theta_L-\theta_U)$. (*b*) Response time as a function of $\Delta\theta_s$.

regimes. In the regime of weak anchoring, the extrapolation length is larger than the cell thickness, *d*, and the response time is small. As seen in figure 5, the response time increases with the anchoring energy and saturates on reaching the strong anchoring regime where the extrapolation length is much smaller than *d*. The influence of asymmetry in the anchoring energy strengths on the response time is illustrated in figure 6 where the anchoring strength at the upper substrate is kept constant at the value listed in the table, $W_U=W$. It is shown that the response time varies slowly and reaches its maximum at $W_L/W_U\approx4.0$.

The surface rotational viscosity, γ_s, can be conveniently characterized by the ratio of γ_s and the bulk viscosity which has the dimension of length. There are, however, only few measurements of this length which, according to [35, 36, 42], can be of the order tens and hundreds of nanometers. Our numerical results on the surface viscosity dependence of the response time are given in figure 7. It can be seen that variations of the
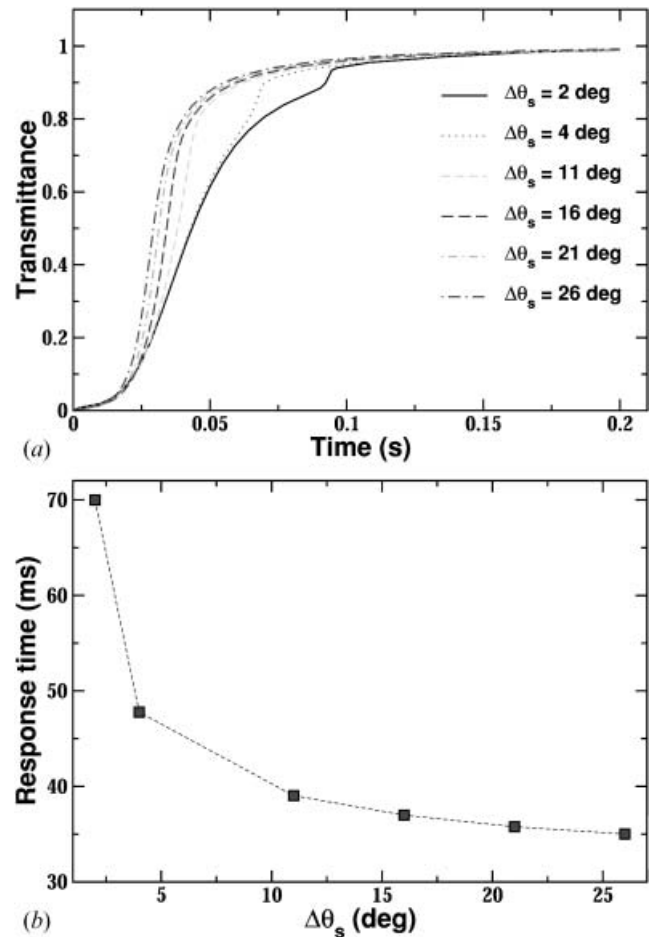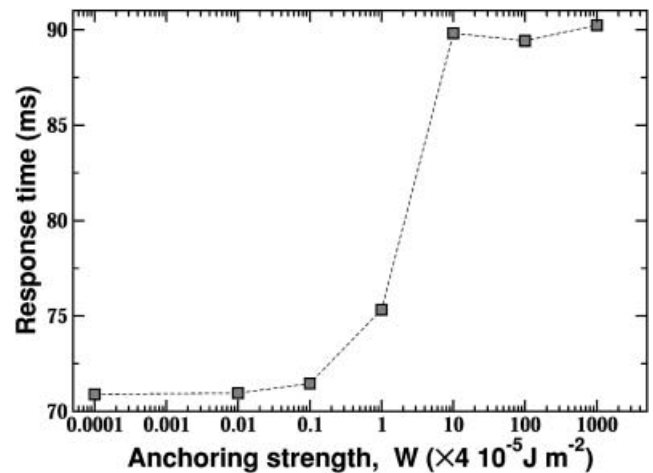

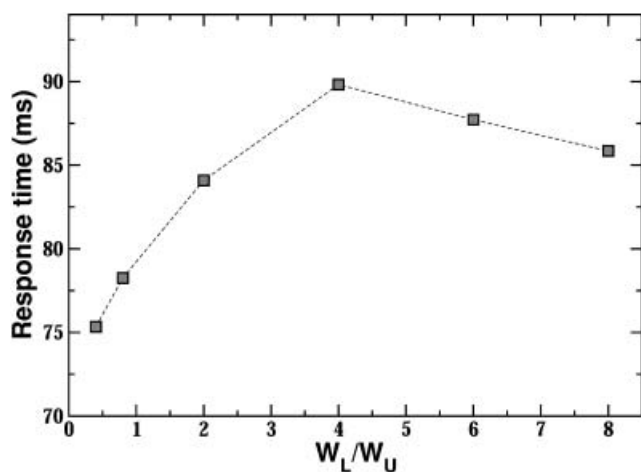Figure 5. Response time as a function of the anchoring strength, $W=W_L=W_U$.

Figure 6. Response time as a function of the anchoring strength ratio, W_L/W_U, at $W_U=W=4.0\times10^{-4}\,\mathrm{J\,m^{-2}}$.
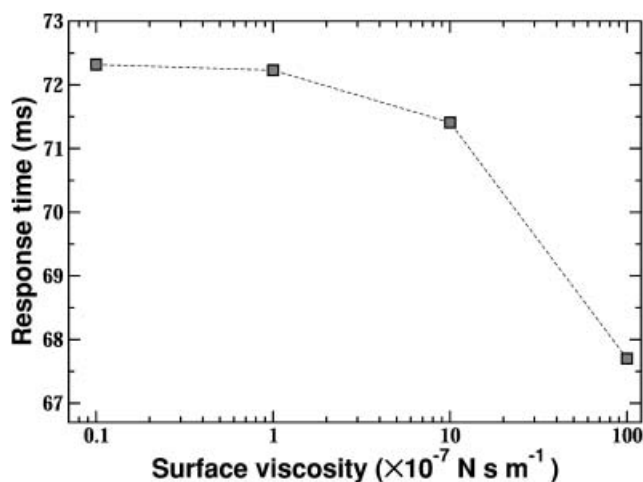

Figure 7. Response time as a function of the rotational surface viscosity.

surface viscosity over a wide range of values have almost no effect on the response time.

So far we have limited our discussion to the case in which the flexoelectric coefficient e_f vanishes and thus the flexoelectric effect appears to be eliminated. There have been measurements of the flexoelectric coefficient in a variety of liquid crystals [43–48]. It was found that the value of $|e_f|$ typically falls in the range 5×10^{-12} to $9\times10^{-11}\,\mathrm{C\,m^{-1}}$. But reliable and accurate experimental estimates of e_f are still needed. For example, the reported values of e_f for MBBA proved to differ in both magnitude and sign depending on the theoretical approach used for processing experimental data [22, 27, 43, 45].

Numerical results related to the effect of flexoelectricity on the dynamics of a NLC cell are given in figures 8–10. The curves shown in figure 8 indicate that the dielectric anisotropy dependence of the response time is strongly affected by the flexoelectric effect. In the presence of flexoelectricity the curve has a pronounced maximum peaked at $u\approx0.5$ which follows a minimum reached at $u\approx0.35$.

By contrast to the dielectric anisotropy dependence, the dependences of the response time on the pretilt angle difference, $\Delta\theta_s$, shown in figure 9, do not differ significantly. For $\Delta\theta_s$ larger than $10°$ see figure 9, the curve with a non-zero flexoelectric coefficient is shifted upward by approximately 5 ms with respect to the curve computed at vanishing e_f.

Finally, we comment on the dependences seen in figure 10. The curves plotted in figure 10 (*a*) represent the temporal evolution of the transmittance at different values of the flexoelectric coefficient. The response time in relation to the flexoelectric coefficient obtained from
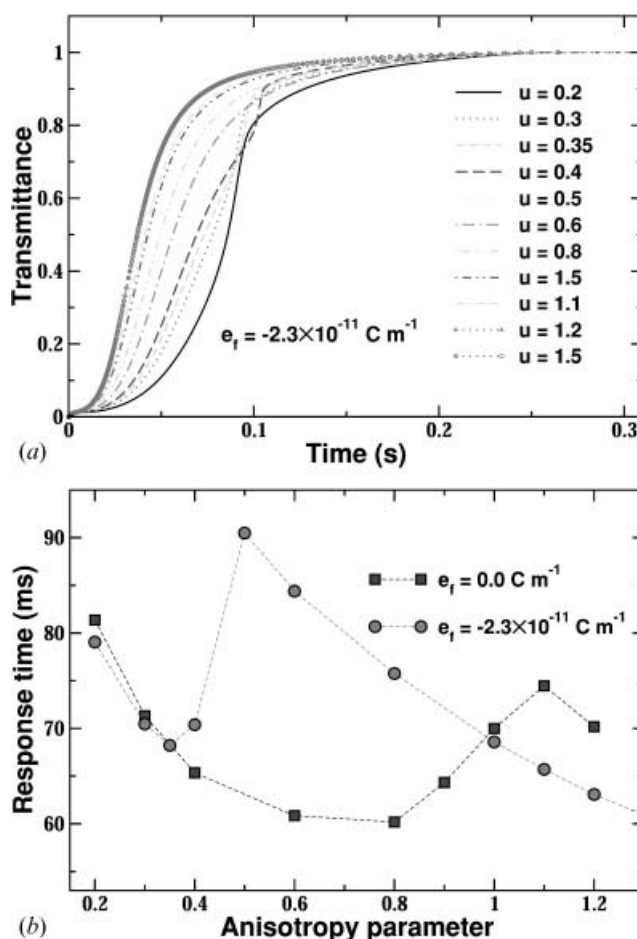

Figure 8. (*a*) Transmittance as a function of time for various values of the dielectric anisotropy parameter at non-vanishing flexoelectric coefficient e_f. (*b*) Response time as a function of u at $e_f=0.0\,\mathrm{C\,m^{-1}}$ (squares) and $e_f=-2.3\times10^{-12}\,\mathrm{C\,m^{-1}}$ (circles).
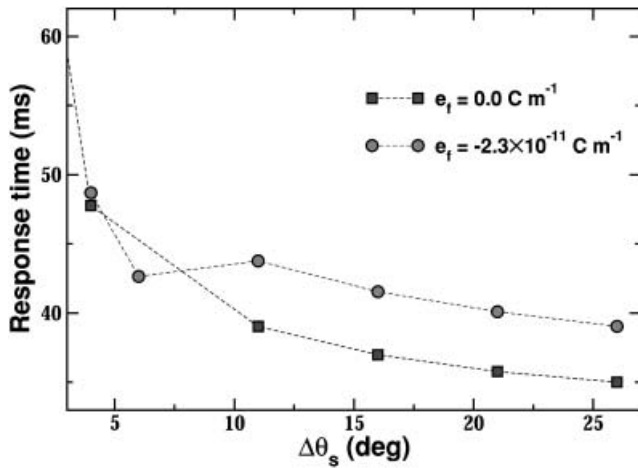
Figure 9. Response time as a function of the pretilt angle difference at $e_f = 0.0 \, \text{C} \, \text{m}^{-1}$ (squares) and $e_f = -2.3 \times 10^{-12} \, \text{C} \, \text{m}^{-1}$ (circles).
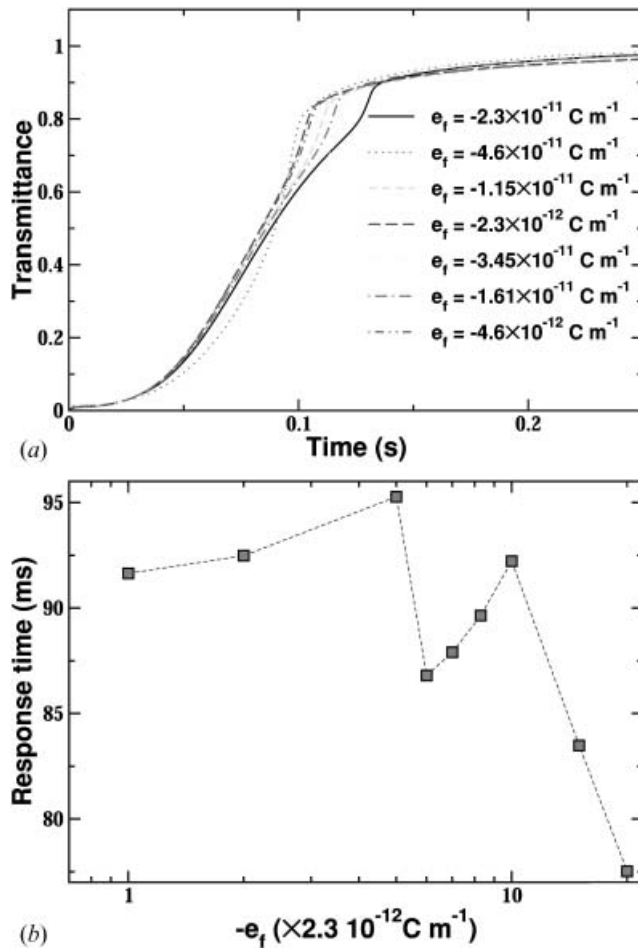

Figure 10. (*a*) Transmittance as a function of time at various values of the flexoelectric coefficient e_f. (*b*) Response time as a function of the flexoelectric coefficient.

these curves is shown in figure 10 (*b*). It can be seen that the response time steeply declines after reaching a maximum at $e_f \approx -1.15 \times 10^{-11} \, \text{C} \, \text{m}^{-1}$.

4. Conclusion

In this work we used a simplified approach to study the dynamics of the optical response at the splay–bend transition that occurs after applying a voltage across a NLC cell. It is assumed that the coupling between the director and the flow velocity can be neglected. A similar approach was recently applied to formulate a model of the switching in a zenithally bistable device [15]. In our case, however, not only the boundary conditions (16) are different, but also the inhomogeneity of the electric field is taken into account using the constitutive relationship (9).

Simulation results for the transmittance were obtained by solving the dynamic equations of the model numerically. The response time characterizing the rate of change of the transmittance was evaluated to study how the parameters of the cell influence the dynamics of optical response. Dependences of the response time on the dielectric anisotropy parameter and on the flexo-electric coefficient are found to be strongly non-monotonic. It was shown that the response time declines as the elastic ratio K_{33}/K_{11} or the pretilt angle difference $\Delta\theta_s$ increase. By contrast, the response time appears to be relatively insensitive to anchoring strength asymmetry and to changes in the surface viscosity.

References

[1] D.W. Berreman, W.R. Heffner. *J. appl. Phys.*, **52**, 3032 (1981).
[2] Z.L. Xie, H.S. Kwok. *J. appl. Phys.*, **84**, 77 (1998).
[3] Z. Zhuang, Y.J. Kim, J.S. Patel. *Appl. Phys. Lett.*, **75**, 3008 (1999).
[4] Z.L. Xie, Y.M. Dong, S.Y. Xu, H.J. Gao, H.S. Kwok. *J. appl. Phys.*, **87**, 2673 (2000).
[5] Z.L. Xie, C.Y. Zheng, S.Y. Xu, H.J. Gao, H.S. Kwok. *J. appl. Phys.*, **88**, 1722 (2000).
[6] J.X. Guo, Z.G. Meng, M. Wong, H.S. Kwok. *Appl. Phys. Lett.*, **77**, 3716 (2000).
[7] J. Cheng, R.N. Thurston, D.W. Berreman. *J. appl. Phys.*, **52**, 2756 (1981).
[8] E.J. Acosta, M.J. Towler, H.G. Walton. *Liq. Cryst.*, **27**, 977 (2000).
[9] H. Nakamura, M. Noguchi. *Jpn. J. appl. Phys.*, **39**, 6368 (2000).
[10] S.H. Lee, T.J. Kim, G.D. Lee, T.H. Yoon, J.C. Kim. *Jpn. J. appl. Phys.*, **42**, L1148 (2003).

[11] I. Inoue, T. Miyashita, T. Uchida, Y. Yamada, Y. Ishii. *J. SID*, **11/3**, 571 (2003).

[12] G. Porte, J.P. Jadot. *J. Phys. (Paris)*, **39**, 213 (1978).

[13] L. Komitov, G. Hauck, H.D. Koswig. *Phys. Stat. Sol.*, **97**, 645 (1986).

[14] H. Cheng, H. Gao. *Liq. Cryst.*, **28**, 1337 (2001).

[15] A.J. Davidson, N.J. Mottram. *Phys. Rev. E*, **65**, 051710 (2002).

[16] H. Cheng, H. Gao. *Liq. Cryst.*, **30**, 839 (2003).

[17] V.I. Tsoy. *Techn. Phys.*, **47**, 34 (2002).

[18] P.J. Kedney, F.M. Leslie. *Liq. Cryst.*, **24**, 613 (1998).

[19] A. Rapini, M. Papoular. *J. Phys. (Paris) Colloq. C4*, **30**, 54 (1969).

[20] P.G. De Gennes, J. Prost. *The Physics of Liquid Crystals*. Clarendon Press, Oxford (1993).

[21] R.B. Meyer. *Phys. Rev. Lett.*, **22**, 918 (1969).

[22] N.T. Kirkman, T. Stirner, W.E. Hagston. *Liq. Cryst.*, **30**, 1115 (2003).

[23] R.N. Thurston, D.W. Berreman. *J. appl. Phys.*, **52**, 508 (1981).

[24] J.F. Palierne. *Phys. Rev. Lett.*, **56**, 1160 (1986).

[25] G. Barbero, G. Durand. *Phys. Rev. A*, **35**, 1294 (1987).

[26] G. Barbero, G. Durand. *J. appl. Phys.*, **68**, 5549 (1990).

[27] S. Ponti, P. Ziherl, C. Ferrero, S. Žumer. *Liq. Cryst.*, **26**, 1171 (1999).

[28] C.V. Brown, N.J. Mottram. *Phys. Rev. E*, **68**, 031702 (2003).

[29] M. Felczak, G. Derfel. *Liq. Cryst.*, **30**, 739 (2003).

[30] P.C. Hohenberg, B.I. Halperin. *Rev. mod. Phys.*, **49**, 435 (1977).

[31] P.M. Chaikin, T.C. Lubensky. *Principles of Condensed Matter Physics*. Cambridge University Press, Cambridge (1995).

[32] P. Pieransky, F. Brochard, E. Guyon. *J. Phys. (Paris)*, **34**, 35 (1973).

[33] D.W. Berreman. *J. appl. Phys.*, **46**, 3746 (1975).

[34] S.M. Chen, T.C. Hsieh. *Phys. Rev. A*, **43**, 2848 (1991).

[35] A. Mertelj, M. Čopič. *Phys. Rev. E*, **61**, 1622 (2000).

[36] M. Vilfan, I.D. Olenik, A. Mertelj, M. Čopič. *Phys. Rev. E*, **63**, 061709 (2001).

[37] P. Ziherl, S. Žumer. *Phys. Rev. E*, **54**, 1592 (1996).

[38] A.M. Sonnet, E.G. Virga, G. Durand. *Phys. Rev. E*, **62**, 3694 (2000).

[39] G. Durand, E.G. Virga. *Phys. Rev. E*, **59**, 4137 (1999).

[40] L.M. Blinov, V.G. Chigrinov. *Electrooptic Effects in Liquid Crystal Materials*. Springer-Verlag, New York (1994).

[41] C.R. Jones. *J. opt. Soc. Am.*, **32**, 486 (1942).

[42] A.G. Petrov, A.T. Ionescu, C. Versace, M. Scaramuzza. *Liq. Cryst.*, **19**, 169 (1995).

[43] N.V. Madhusudana, G. Durand. *J. Phys. (Paris) Lett.*, **46**, L195 (1985).

[44] S.R. Warrier, N.V. Madhusudana. *J. Phys. II*, **7**, 1789 (1997).

[45] T. Takahashi, S. Hashidate, H. Nishijou, M. Usui, M. Kimura, T. Akahane. *Jpn. J. appl. Phys.*, **37**, 1865 (1998).

[46] L.M. Blinov, M.I. Barnik, H. Ohoka, M. Ozaki, K. Yoshino. *Phys. Rev. E*, **64**, 031707 (2001).

[47] A. Mazzulla, F. Ciuchi, J.R. Sambles. *Phys. Rev. E*, **64**, 021708 (2001).

[48] S.A. Jewel, J.R. Sambles. *J. appl. Phys.*, **92**, 19 (2002).